**Література**

1. Плоткин Е. Р., Лейзерович А. Ш. Пусковые режимы паровых турбин энергоблоков. М.: Энергия, 1980. 192 с.
2. Зарянкин А. Е., Симонов Б. П. Регулирующие и стопорно-регулирующие клапана паровых турбин. М.: Моск. энерг. ин-т, 2005. 360 с.
3. Menter, F. R. Eddy Viscosity Transport Equations and their Relation to the k–ε Model. *ASME J. Fluids Eng.* 1997. Vol. 119. Iss. 4. P. 876–884. https://doi.org/10.1115/1.2819511
4. Колядюк А. С., Шульженко Н. Г., Бабаев И. Н. Численное моделирование течения пара в регулировочном клапане турбины. *Вестн. двигателестроения.* 2011. № 2. С. 106–110.
5. Колядюк А. С., Шульженко Н. Г., Ершов С. В. Течение пара и распределение температуры в системе пораспределения турбины для различных режимов ее работы. *Авиац.-косм. техника.* 2012. № 7. С. 85–90.
6. Шульженко Н. Г., Колядюк А. С. Оценка ползучести корпуса регулирующего клапана паровой турбины К-325. *Вісн. НТУ «ХПІ». Сер. Енергетичні та теплотехнічні процеси й устаткування*. 2014. № 11. С. 125–131.
7. ПНАЭ Г-7-002-86. Нормы расчета на прочность оборудования и трубопроводов атомных энергетических установок / Госатомэнергонадзор СССР. М.: Энергоатомиздат, 1989. 525 с.

**DOI: https://doi.org/10.15407/pmach2019.02.044**

UDC 539.3

# INVESTIGATION OF THE STRESS STRAIN STATE OF THE LAYER WITH A LONGITUDINAL CYLINDRICAL THICK-WALLED TUBE AND THE DISPLACEMENTS GIVEN AT THE BOUNDARIES OF THE LAYER

**Vitaliy Yu. Miroshnikov**
m0672628781@gmail.com
ORCID: 0000-0002-9491-0181

Kharkiv National University of Construction and Architecture,
40, Sumska str., Kharkiv, 61002, Ukraine

*This paper proposes an analytical-numerical approach to solving the spatial problem of the theory of elasticity for the layer with a circular cylindrical tube. A cylindrical empty thick-walled tube is located inside the layer parallel to its surfaces and is rigidly fixed to it. It is necessary to investigate the stress-strain state of the elastic bodies of both the layer and tube. Stresses are given on the inner surface of the tube, and displacements, on the boundaries of the layer. The solution to the spatial problem of the theory of elasticity is obtained by the generalized Fourier method with respect to the system of Lamé's equations in the cylindrical coordinates associated with the tube and the Cartesian coordinates associated with the boundaries of the layer. Infinite systems of linear algebraic equations obtained as a result of satisfying the boundary and conjugation conditions are solved by the truncation method. As a result, displacements and stresses are obtained at various points of the elastic layer and elastic tube. Due to the selected truncation parameter for the given geometrical characteristics, the satisfaction of boundary conditions has been brought to $10^{-3}$. An analysis of the stress-strain state for the elastic body at different thicknesses of the tube, as well as at different distances from the tube to the boundaries of the layer is conducted. Graphs of normal and tangential stresses at the boundary of the tube and layer, as well as normal stresses on the inner surface of the tube are presented. These stress graphs indicate that as the tube approaches the upper boundary of the layer, the stresses in the elastic bodies of both the layer and tube increase, and with decreasing tube thickness, the stresses in the elastic body of the layer decrease, growing in the elastic body of the tube. The proposed method can be used to calculate structures and parts, whose design schemes coincide with the formulation of the problem of this paper. The analysis of the stress state can be used to select the geometrical parameters of the designed structure, and the stress graph at the boundary of the tube and layer can be used to analyze the strength of the joint.*

***Keywords**: thick-walled tube in a layer, Lamé's equations, generalized Fourier method.*

## Introduction

When designing composite structures and components whose calculation scheme is the layer with a built-in longitudinal circular tube, it is necessary to have an idea of the stress-strain state of the layer and tubes, as well as the stress in their joint. To achieve this, it is required that there be a method of calculation that would give an opportunity to obtain the result with the necessary accuracy.

In the majority of publications, a plate or layer with a transverse circular cavity or inclusion [1, 2] is considered. However, the methods used therein can not be applied to the layer with a longitudinal cavity or inclusion.

In [3–5], stationary problems of the wave diffraction and determination of stresses are considered for the layer with a longitudinal cylindrical cavity or inclusion on the basis of the Fourier decomposition method. The problem for the layer with a circular cavity perpendicular to the boundaries of the layer, which is solved with the help of the method of superposition of general solutions, is considered in [6].

In [7], with the help of the image method, the boundary value problem of the diffraction of symmetric normal waves of the longitudinal displacement for the layer with a cylindrical cavity or inclusion is solved.

In the work mentioned above, an analytic-numerical approach is used, which is based on the generalized Fourier method [8]. On the basis of this method, problems have been solved for a half-space with a cylindrical cavity or inclusion [9-13], as well as for a cylinder with cylindrical inclusions [14].

**Problem Formulation**

In the elastic homogeneous layer, there is a circular cylindrical thick-walled tube with an external radius $R_1$ and internal radius $R_2$ (Fig. 1).

The tube will be considered in the cylindrical coordinate system (ρ, φ, z), the boundary of the layer in the Cartesian coordinate system ($x$, $y$, $z$), which is equally oriented and connected with the tube coordinate system (Fig. 1). The upper boundary of the layer is located at the distance $y=h$, and the lower one, at the distance $y=-\tilde{h}$ . It is necessary to find a solution to the Lamé equation on condition that at the boundaries of the layer, the displacements $\vec{U}_1(x,z)_{|y=h} = \vec{U}_h^0(x,z)$, $\vec{U}_1(x,z)_{|y=-\tilde{h}} = \vec{U}_{\tilde{h}}^0(x,z)$ are given, on the inner surface of the tube, the stresses $F\vec{U}_2(\varphi,z)_{|\rho=R_2} = \vec{F}_R^0(\varphi,z)$, and at the boundary of the tube and layer, the conjugation conditions

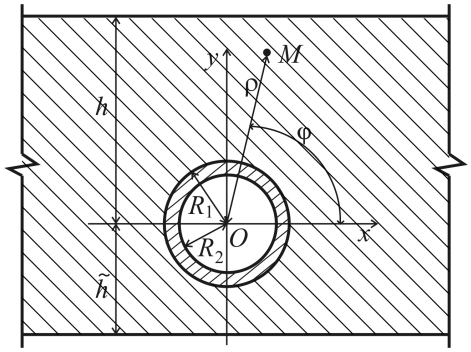


***Fig. 1. Layer with a cylindrical tube***

$$\vec{U}_1(\varphi,z)_{|\rho=R_1} = \vec{U}_2(\varphi,z)_{|\rho=R_1}, \quad (1)$$

$$F\vec{U}_1(\varphi,z)_{|\rho=R_1} = F\vec{U}_2(\varphi,z)_{|\rho=R_1}, \quad (2)$$

where $\vec{U}_1$ is the displacement in the layer; $\vec{U}_2$ is the displacement in the tube; $F\vec{U} = 2\cdot G\cdot\left[\frac{\sigma}{1-2\cdot\sigma}\vec{n}\cdot\operatorname{div}\vec{U} + \frac{\partial}{\partial n}\vec{U} + \frac{1}{2}\left(\vec{n}\times\operatorname{rot}\vec{U}\right)\right]$ is the stress operator;

$$\begin{aligned}
\vec{U}_h^0(x,z) &= U_x^{(h)}\vec{e}_1^{(1)} + U_y^{(h)}\vec{e}_2^{(1)} + U_z^{(h)}\vec{e}_3^{(1)},\\
\vec{U}_{\tilde{h}}^0(x,z) &= U_x^{(\tilde{h})}\vec{e}_1^{(1)} + U_y^{(\tilde{h})}\vec{e}_2^{(1)} + U_z^{(\tilde{h})}\vec{e}_3^{(1)},\\
\vec{F}_R^0(\varphi,z) &= \sigma_\rho^{(p)}\vec{e}_1^{(2)} + \tau_{\rho\varphi}^{(p)}\vec{e}_2^{(2)} + \tau_{\rho z}^{(p)}\vec{e}_3^{(2)}
\end{aligned} \quad (3)$$

are known functions; $\vec{e}_j^{(k)}$, $(j=1,2,3)$ are the unit vectors of the Cartesian ($k$=1) and cylindrical ($k$=2) coordinate systems; σ, $G$ are elastic constants.

All the given vectors and functions will be considered fast falling to zero at great distances from the origin of the $z$ coordinate for the tube and the x and $z$ coordinates for the boundaries of the layer.

**Solving the Problem**

Choose the basic solutions to the Lamé equation for the specified coordinate systems in the form [8]

$$\begin{aligned}
\vec{u}_k^{\pm}(x,y,z;\lambda,\mu) &= N_k^{(d)}e^{i(\lambda z+\mu x)\pm\gamma y};\\
\vec{R}_{k,m}(\rho,\varphi,z;\lambda) &= N_k^{(p)}I_m(\lambda\rho)e^{i(\lambda z+m\varphi)};\\
\vec{S}_{k,m}(\rho,\varphi,z;\lambda) &= N_k^{(p)}\left[(\operatorname{sign}\lambda)^m K_m(|\lambda|\rho)\cdot e^{i(\lambda z+m\varphi)}\right], k=1,2,3;
\end{aligned} \quad (4)$$

$$N_1^{(d)}=\frac{1}{\lambda}\nabla;\ N_2^{(d)}=\frac{4}{\lambda}(\sigma-1)\vec{e}_2^{(1)}+\frac{1}{\lambda}\nabla(y\cdot);\ N_3^{(d)}=\frac{i}{\lambda}\mathrm{rot}(\vec{e}_3^{(1)}\cdot);\ N_1^{(p)}=\frac{1}{\lambda}\nabla;$$

$$N_2^{(p)}=\frac{1}{\lambda}\left[\nabla\left(\rho\frac{\partial}{\partial\rho}\right)+4(\sigma-1)\left(\nabla-\vec{e}_3^{(2)}\frac{\partial}{\partial z}\right)\right];\ N_3^{(p)}=\frac{i}{\lambda}\mathrm{rot}(\vec{e}_3^{(2)}\cdot);\ \gamma=\sqrt{\lambda^2+\mu^2},\ -\infty<\lambda,\mu<\infty,$$

where $\sigma$ is the Poisson factor; $I_m(x)$, $K_m(x)$ are the modified Bessel functions; $\vec{R}_{k,m}$, $\vec{S}_{k,m}$, $k$=1, 2, 3 are, respectively, the internal and external solutions to the Lamé equation for the cylinder; $\vec{u}_k^{(-)}$, $\vec{u}_k^{(+)}$ are the solutions to the Lamé equation for the layer.

The solution to the problem will be presented in the form

$$\vec{U}_1=\sum_{k=1}^{3}\int_{-\infty}^{\infty}\sum_{m=-\infty}^{\infty}B_{k,m}(\lambda)\cdot\vec{S}_{k,m}(\rho,\varphi,z;\lambda)d\lambda+$$
$$+\sum_{k=1}^{3}\int_{-\infty}^{\infty}\int_{-\infty}^{\infty}\left(H_k(\lambda,\mu)\cdot\vec{u}_k^{(+)}(x,y,z;\lambda,\mu)+\tilde{H}_k(\lambda,\mu)\cdot\vec{u}_k^{(-)}(x,y,z;\lambda,\mu)\right)d\mu d\lambda, \tag{5}$$

$$\vec{U}_2=\sum_{k=1}^{3}\int_{-\infty}^{\infty}\sum_{m=-\infty}^{\infty}A_{k,m}(\lambda)\cdot\vec{R}_{k,m}(\rho,\varphi,z;\lambda)+\tilde{A}_{k,m}(\lambda)\cdot\vec{S}_{k,m}(\rho,\varphi,z;\lambda)d\lambda, \tag{6}$$

where, $\vec{S}_{k,m}(\rho,\varphi,z;\lambda)$, $\vec{R}_{k,m}(\rho,\varphi,z;\lambda)$ $\vec{u}_k^{(+)}(x,y,z;\lambda,\mu)$ and $\vec{u}_k^{(-)}(x,y,z;\lambda,\mu)$ are the basic solutions given by formulas (4), and the unknown functions $H_k(\lambda,\mu)$, $\tilde{H}_k(\lambda,\mu)$, $B_{k,m}(\lambda)$, $A_{k,m}(\lambda)$, and $\tilde{A}_{k,m}(\lambda)$ must be found from the boundary conditions (3) and conjugation conditions (1) and (2).

To switch between the coordinate systems (Fig. 1), we use formulas

– for the transition from the solutions $\vec{S}_{k,m}$ of the cylindrical coordinate system to the solutions for the layer $\vec{u}_k^{(-)}$ (at $y$>0) and $\vec{u}_k^{(+)}$ (at $y$<0)

$$\vec{S}_{k,m}(\rho,\varphi,z;\lambda)=\frac{(-i)^m}{2}\int_{-\infty}^{\infty}\omega_{\mp}^m\cdot\vec{u}_k^{(\mp)}\cdot\frac{d\mu}{\gamma},\ k=1,\ 3;$$
$$\vec{S}_{2,m}(\rho,\varphi,z;\lambda)=\frac{(-i)^m}{2}\int_{-\infty}^{\infty}\omega_{\mp}^m\cdot\left(\left(\pm m\cdot\mu-\frac{\lambda^2}{\gamma}\right)\vec{u}_1^{(\mp)}-\lambda^2\vec{u}_2^{(\mp)}\pm 4\mu(1-\sigma)\vec{u}_3^{(\mp)}\right)\frac{d\mu}{\gamma^2}, \tag{7}$$

where $\gamma=\sqrt{\lambda^2+\mu^2}$, $\omega_{\mp}(\lambda,\mu)=\dfrac{\mu\mp\gamma}{\lambda}$, $m=0,\pm1,\pm2,\ldots$;

– for the transition from the solutions $\vec{u}_k^{(+)}$ and $\vec{u}_k^{(-)}$ for the layer to the solutions $\vec{R}_{k,m}$ of the cylindrical coordinate system

$$\vec{u}_k^{(\pm)}(x,y,z)=\sum_{m=-\infty}^{\infty}(i\cdot\omega_{\mp})^m\vec{R}_{k,m},\ (k=1,\ 3);$$
$$\vec{u}_2^{(\pm)}(x,y,z)=\sum_{m=-\infty}^{\infty}\left[(i\cdot\omega_{\mp})^m\cdot\lambda^{-2}\left((m\cdot\mu)\cdot\vec{R}_{1,m}\pm\gamma\cdot\vec{R}_{2,m}+4\mu(1-\sigma)\vec{R}_{3,m}\right)\right], \tag{8}$$

where $\vec{R}_{k,m}=\vec{\tilde{b}}_{k,m}(\rho,\lambda)\cdot e^{i(m\varphi+\lambda z)}$;

$$\vec{\tilde{b}}_{1,n}(\rho,\lambda)=\vec{e}_\rho\cdot I_n'(\lambda\rho)+i\cdot I_n(\lambda\rho)\cdot\left(\vec{e}_\varphi\frac{n}{\lambda\rho}+\vec{e}_z\right);$$

$$\vec{\tilde{b}}_{2,n}(\rho,\lambda)=\vec{e}_\rho\cdot\left[(4\sigma-3)\cdot I_n'(\lambda\rho)+\lambda\rho_p I_n''(\lambda\rho)\right]+\vec{e}_\varphi i\cdot m\left(I_n'(\lambda\rho)+\frac{4(\sigma-1)}{\lambda\rho}I_n(\lambda\rho)\right)+\vec{e}_z i\lambda\rho I_n'(\lambda\rho);$$

$$\vec{\tilde{b}}_{3,n}(\rho,\lambda)=-\left[\vec{e}_\rho\cdot I_n(\lambda\rho)\frac{n}{\lambda\rho}+\vec{e}_\varphi\cdot i\cdot I_n'(\lambda\rho)\right],$$

$\vec{e}_\rho$, $\vec{e}_\varphi$, $\vec{e}_z$ are the unit vectors in the cylindrical coordinate system.

To satisfy the boundary conditions at the boundaries of the layer, $y=h$ and $y=-\tilde{h}$, using the transition formulas (7), we rewrite the vectors $\vec{S}_{k,m}$ in (5) in the Cartesian coordinate system through using the basic solutions $\vec{u}_k^{(-)}$ and $\vec{u}_k^{(+)}$, respectively. We then equate the resulting vectors (at $y=h$ and at $y=-\tilde{h}$) to the given vectors $\vec{U}_h^0(x,z)$ and $\vec{U}_{\tilde{h}}^0(x,z)$, represented by the double Fourier integral.

The resulting system of 6 equations has the determinant

$$\frac{4\cdot e^{-x}\cdot\gamma^2\cdot\left(e^{2x}-1\right)\left(x^2-\overline{\sigma}^2\cdot\mathrm{sh}^2\,x\right)}{\lambda^4}$$

where $x=\gamma\left(h+\tilde{h}\right)$, $\overline{\sigma}=3-4\sigma$.

From the obtained equations we obtain the functions $H_k(\lambda,\mu)$ and $\tilde{H}_k(\lambda,\mu)$ through $B_{k,m}(\lambda)$.

To take into account the conjugation conditions (1), we decompose the basic solutions $\vec{u}_k^{(\pm)}$ in (5) by means of (8), turning them into the solutions $\vec{R}_{k,m}$. We then equate $\rho=R_1$ therein. This will satisfy condition (1).

To take into account the conjugation conditions (2), we obtain the vectors $F\vec{U}_1$ and $F\vec{U}_2$ from solution (6) and the solution decomposed through $\vec{u}_k^{(\pm)}$ (5). We then equate $\rho=R_1$ therein. This will satisfy condition (2).

These two conditions give 6 equations, connecting all the unknowns in equations (5), (6).

Another three equations are given by the condition on the inner surface of the tube. To satisfy the boundary conditions on this surface, we apply the stress operator to the right-hand side of (6), and equate (at $\rho=R_2$) to $\vec{F}_R^0(\varphi,z)$ given by both the integral and Fourier series.

From this system of nine equations, we will exclude the functions $H_k(\lambda,\mu)$ and $\tilde{H}_k(\lambda,\mu)$ previously obtained through $B_{k,m}(\lambda)$. Having gotten rid of the series $m$ and integrals $\lambda$, we obtain a system of nine infinite systems of linear algebraic equations for identifying the unknowns $A_{k,m}(\lambda)$, $\tilde{A}_{k,m}(\lambda)$, and $B_{k,m}(\lambda)$.

To the obtained infinite systems of equations, we will apply the truncation method. The numerical studies have shown that the determinant of the truncated system does not turn to zero at any $m$, for $0\le m\le 10$, which is why this system of equations has a unique solution.

Having solved this system, we will find the unknowns $A_{k,m}(\lambda)$, $\tilde{A}_{k,m}(\lambda)$, and $B_{k,m}(\lambda)$.

We will substitute the functions $B_{k,m}(\lambda)$ obtained from the infinite system of equations into $H_k(\lambda,\mu)$ and $\tilde{H}_k(\lambda,\mu)$. This will identify all unknown tasks.

**Numerical Studies of Stressed State**

We have a layer with a longitudinal cylindrical tube (Fig. 1). Both the layer and tube are made of isotropic materials: for the layer, Poisson's coefficient $\sigma_1=0.38$, the modulus of elasticity $E_1=1700$ N/mm$^2$; for the tube, Poisson's coefficient $\sigma_2=0.21$, the modulus of elasticity $E_2=200\,000$ N/mm$^2$. The outer radius of the tube $R_1=10$ mm. The internal one was calculated in two variants, namely $R_2=6$ mm and $R_2=8$ mm. The thickness of the layer $h+\tilde{h}=60$ mm. The distance from the upper boundary of the layer to the center of the tube was calculated in two variants, namely $h=30$ mm and $h=20$ mm.

At the upper boundary of the layer, the displacements $U_y^{(h)}(x,z)=-10^8\cdot\left(z^2+10^2\right)^{-2}\cdot\left(x^2+10^2\right)^{-2}$, $U_x^{(h)}=U_z^{(h)}=0$ are given; at the lower boundary of the layer, the displacements $U_x^{(\tilde{h})}=U_y^{(\tilde{h})}=U_z^{(\tilde{h})}=0$; on the inner surface of the tube, the stresses $\sigma_\rho^{(p)}=\tau_{\rho\varphi}^{(p)}=\tau_{\rho z}^{(p)}=0$.

A finite system of equations of order $m$=10 was solved. The calculations of integrals were performed using Filon's quadrature formulas (for oscillating functions) and Simpson's quadrature formulas (for non-oscillating functions). The accuracy of the implementation of the boundary conditions for the indicated values of geometric parameters was $10^{-3}$.

At the upper boundary of the layer, at $z$=0, the maximum stress is the following: at $h$=30 mm, $R_2$=6 mm, $\sigma_\rho$ = -246.42 N/mm$^2$; at $h$=20 mm, $R_2$=6 mm, $\sigma_\rho$ = -283.29 N/mm$^2$; at $h$=30 mm, $R_2$=8 mm $\sigma_\rho$ = 244.71 N/mm$^2$; at $h$=20 mm, $R_2$=8 mm, $\sigma_\rho$ = -272.25 N/mm$^2$. This indicates that with the approach of the cylindrical tube to the boundary of the layer, the stresses $\sigma_\rho$ on the surface of the layer increase, and with a decrease in the thickness of the tube, these stresses decrease.

Fig. 2 shows the stresses (in N/mm$^2$ ) at the boundary of the tube and layer in the plane $z$=0 in the elastic body of the layer. The stresses $\sigma_\rho$ , $\sigma_\varphi$ at $3\pi/4<\varphi<\pi/4$ and $\tau_{\rho z}$ at $\varphi>\pi$ have small values, so on the graph they are not shown. The stress graph $\sigma_z$ has the same form as the stress graph $\sigma_\varphi$ , and differs little in values.

The stresses $\sigma_\rho$ , $\sigma_\varphi$ at the boundary of the tube and layer (Fig. 2, a, b) increase with the approach of the tube to the upper boundary of the layer (line 1 goes into line 2, line 3 goes into line 4). As the thickness of the tube decreases, the stresses decrease (line 1 goes into line 3, line 2 goes into line 4). The tangential stresses $\tau_{\rho z}$ at the boundary of the tube and layer (Fig. 2, c) are almost independent of the thickness of the tube (on the graph, lines 1 and 3, and lines 2 and 4 coincide), while with the tube approaching the upper boundary of the layer, these stresses increase (line 1 goes into line 2).

Fig. 3 shows the stresses (in N/mm$^2$) at the boundary of the tube and layer in the plane $z$=0 in the elastic body of the tube. They differ significantly from the stresses in the elastic body of the layer because of the difference in the materials of which the layer and tube are made.

With the approach of the tube to the upper boundary of the layer or with a decrease in the thickness of the tube, the stresses $\sigma_\varphi$ on the outer surface of the tube (Fig. 3, a) increase.

The stresses $\sigma_z$ in the upper part of the tube (Fig. 3, b, $\varphi$=0…$\pi$) change with the same principle as the stresses $\sigma_\varphi$. In the lower part of the tube, with a decrease in its thickness, the stresses $\sigma_z$ decrease (line 1 goes into line 3, line 2 goes into line 4).

Fig. 4 shows the stresses $\sigma_\varphi$ and $\sigma_z$ (in N/mm$^2$) on the inner surface of the tube in the plane $z$=0.

The stresses $\sigma_\varphi$ (Fig. 4, a) along the whole radius, in comparison with those on the outer surface of the tube, have opposite sign val-

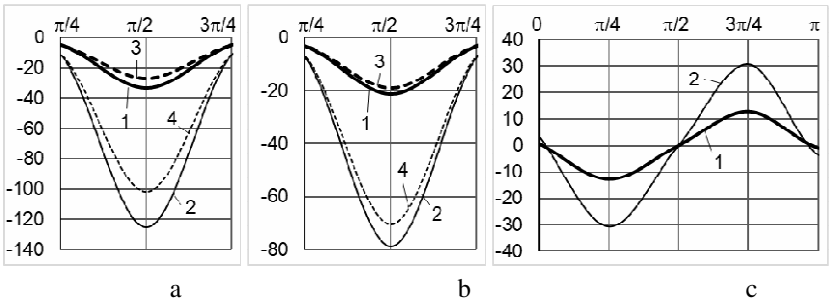


a b c

***Fig. 2. Stresses at the boundary of the tube and layer (in the elastic body of the layer):***

a – $\sigma_\rho$ ; b – $\sigma_\varphi$ ; c – $\tau_{\rho z}$ ;

1 – at $h$=30 mm, $R_2$=6 mm; 2 – at $h$=20 mm, $R_2$=6 mm;
3 – at $h$=30 mm, $R_2$=8 mm; 4 – at $h$=20 mm, $R_2$=8 mm

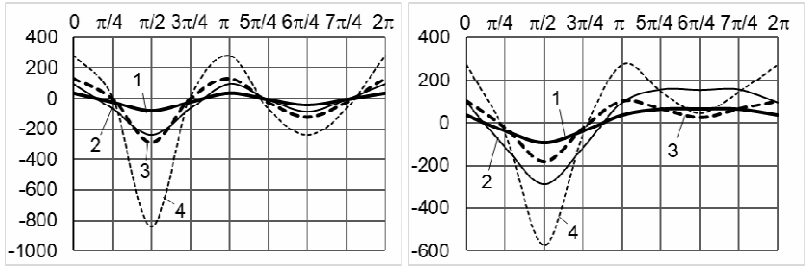


a b

***Fig. 3. Stresses at the boundary of the tube and layer (in the elastic body of the tube):***

a – $\sigma_\varphi$ ; b – $\sigma_z$ ;

1 – at $h$=30 mm, $R_2$=6 mm; 2 – at $h$=20 mm, $R_2$=6 mm;
3 – at $h$=30 mm, $R_2$=8 mm; 4 – at $h$=20 mm, $R_2$=8 mm

ues. The stresses $\sigma_z$ (Fig. 4, b), in comparison with those on the outer surface, in the upper part of the tube, have opposite sign values, and in the lower part of the tube increase with a decrease in the thickness of the tube or the approach of the tube to the upper boundary.

With the approach of the tube to the upper boundary of the layer, or with a decrease in the thickness of the tube, the stresses $\sigma_\varphi$ and $\sigma_z$ increase.

Fig. 5 shows the stresses $\sigma_\rho$, $\sigma_\varphi$, and $\tau_{\rho z}$ (in N/mm$^2$) along the $z$ axis at the boundary of the tube and layer (in the elastic body of the layer) at $\varphi=\pi/2$. The stress graph $\sigma_z$ has the same form as the stress graph $\sigma_\varphi$, and differs little in values.

Figs. 5, a and 5, b clearly show that with the approach of the tube to the upper boundary of the layer, the stresses $\sigma_\rho$ and $\sigma_\varphi$ along the $z$ axis, in addition to negative values, also have positive values. The stresses $\tau_{\rho z}$ at the boundary of the tube and layer (Fig. 5) do not depend on the thickness of the tube (line 3 coincides with line 1, line 4 coincides with line 2).

Fig. 6 shows the stresses $\sigma_\varphi$ and $\sigma_z$ (in N/mm$^2$) along the $z$ axis at the boundary of the tube and layer (in the elastic body of the tube) at $\varphi=\pi/2$.

Fig. 6, a clearly shows that the stresses $\sigma_\varphi$ at the boundary of the tube and layer in the elastic body of the tube, regardless of the distance from the tube to the upper boundary of the layer, constantly have negative values. The stresses $\sigma_z$ along the z axis (Fig. 6, b), irrespective of both the distance of the tube to the upper boundary of the layer and the thickness of the tube, in addition to negative values, also have positive ones that slowly decrease along the $z$ axis.

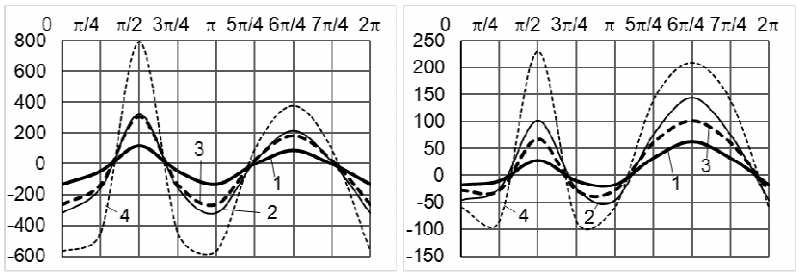


а б

***Fig. 4. Stresses on the inner surface of the tube:***

а – $\sigma_\varphi$; b – $\sigma_z$;

1 – at $h$=30 mm, $R_2$=6 mm; 2 – at $h$=20 mm, $R_2$=6 mm;
3 – at $h$=30 mm, $R_2$=8 mm; 4 – at $h$=20 mm, $R_2$=8 mm

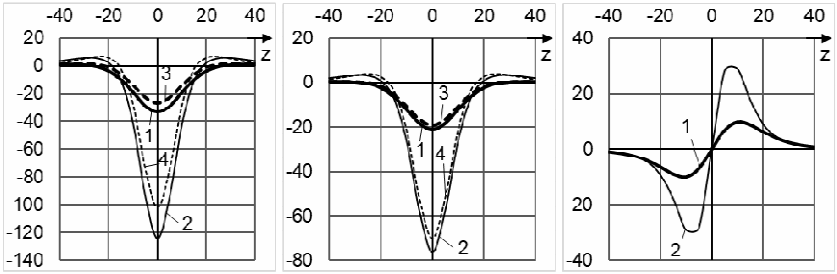


a b c

***Fig. 5. Stresses along the z axis at the boundary of the tube and layer (in the elastic body of the layer):***

а – $\sigma_\rho$; b – $\sigma_\varphi$; c – $\tau_{\rho z}$;

1 – at $h$=30 mm, $R_2$=6 mm; 2 – at $h$=20 mm, $R_2$=6 mm;
3 – at $h$=30 mm, $R_2$=8 mm; 4 – at $h$=20 mm, $R_2$=8 mm

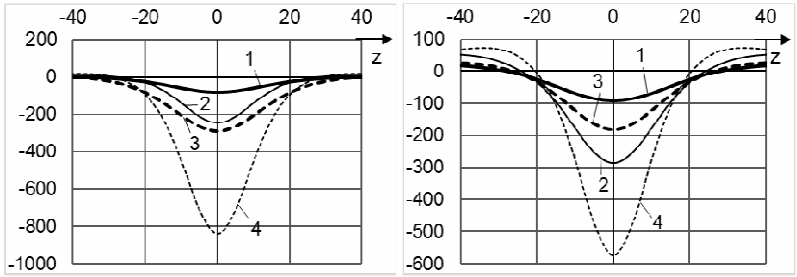


a b

***Fig. 6. Stresses along the z-axis at the boundary of the tube and layer (in the elastic body of the tube):***

а – $\sigma_\varphi$; b – $\sigma_z$;

1 – at $h$=30 mm, $R_2$=6 mm; 2 – at $h$=20 mm, $R_2$=6 mm;
3 – at $h$=30 mm, $R_2$=8 mm; 4 – at $h$=20 mm, $R_2$=8 mm

Fig. 7 shows the stresses $\sigma_\varphi$ and $\sigma_z$ (in N/mm$^2$) along the z axis on the inner surface of the tube at $\varphi=\pi/2$.

The stresses $\sigma_\varphi$ on the inner surface of the tube along the $z$ axis (Fig. 7, a), regardless of the thickness of the tube and distance from the tube to the upper boundary of the layer, are constantly of positive value. The stresses $\sigma_z$ on the same surface (Fig. 7, b), with a decrease in the thickness of the tube, not only increase in value and have the expressed negative values, but also slowly decrease along the $z$ axis.

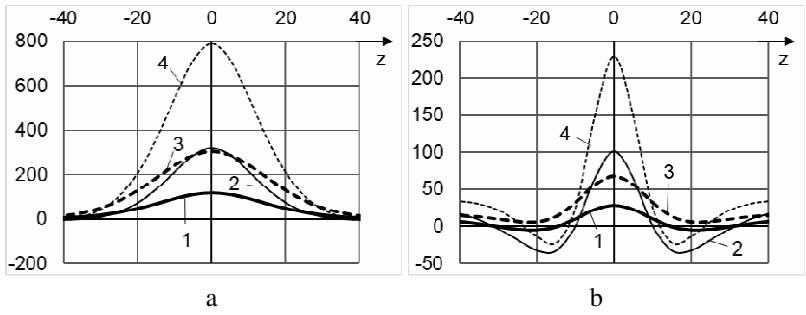


a b

***Fig. 7. Stresses along the z axis on the inner surface of the tube:***
a – $\sigma_\varphi$ ; b – $\sigma_z$ ;
1 – at $h$=30 mm, $R_2$=6 mm; 2 – at $h$=20 mm, $R_2$=6 mm;
3 – at $h$=30 mm, $R_2$=8 mm; 4 – at $h$=20 mm, $R_2$=8 mm

**Conclusions**

With the help of the generalized Fourier method, we developed an analytic-numerical method for calculating the spatial mixed problem of the theory of elasticity (with the conditions of the first and second basic problems at the boundaries) for the layer with a longitudinal, thick-walled tube therein. The problem is reduced to a system of infinite systems of linear algebraic equations.

The equation is solved by the method of reduction to a finite system.

The graphs given present the distribution of stresses on the surfaces of the layer and tube, depending on both the thickness of the tube and distance between the upper boundary of the layer and center of the tube. As a result, the influence of these geometric conditions on the stress-strain state of the layer and tube on the invariable elastic material constants is analyzed.

The stresses $\sigma_\rho$, $\tau_{\rho z}$ obtained at the boundary of the tube and layer can be used to calculate the strength of the joint.

In comparison with works [3–7], the proposed method allows us to obtain the exact solution to the problem in the spatial variant, and, in comparison with [9–15], take into account new boundary surfaces, with the tube and layer junction conditions added to the boundary conditions.

The numerical analysis of the stress-strain state of the layer and the tube therein shows that:

– with the approach of the tube to the upper boundary of the layer, the stresses in the elastic bodies of the layer and tube increase;

– with a decrease in the thickness of the tube, the stresses in the elastic body of the layer decrease, while those in the elastic body of the tube increase;

– with a decrease in the thickness of the tube, the normal stresses along the $z$-axis at the boundary of the tube and layer (in the elastic body of the layer), in addition to negative values, also have positive values.

The numerical studies of the algebraic system for the layer with a longitudinal tube give us an opportunity to assert that its solution can be found with any degree of accuracy by the method of reduction. This is confirmed by the high accuracy of the implementation of the boundary conditions. For the geometric parameters of the solved problem at $m$=10, the boundary conditions are performed with an accuracy of $10^{-3}$. With increasing order of the system, the accuracy of calculations will increase.

To verify the validity of the method, the tube was replaced with a cavity, the lower boundary of the layer was moved a great distance (thus modeling the cavity in a half-space), and in this formulation the results were compared with work [15]. After this, the upper boundary of the layer was moved a great distance (which modeled the cavity in space and coincided with the statement of the problem [16]. Convergence with known results and a high accuracy of the implementation of boundary conditions indicate the reliability of the method and the results obtained.

The resulting graphs can be used to evaluate the stress state in constructions with similar conditions.

However, it should be noted that the method does not allow the problem to be solved when the boundaries of elastic bodies touch or intersect.

A further development of this direction is possible in increasing the number of cylindrical cavities and tubes or in calculating the problem with other boundary conditions.

## References


1. Vaysfeld, N., Popov, G., & Reut, V. (2015). The axisymmetric contact interaction of an infinite elastic plate with an absolutely rigid inclusion. *Acta Mechanica*, vol. 226, iss. 3, pp. 797–810. https://doi.org/10.1007/s00707-014-1229-7.
2. Popov, G. Ya. & Vaysfeld, N. D. (2014). Solving an axisymmetric problem of elasticity for an infinite plate with a cylindrical inclusion with allowance for its specific weight. *International Applied Mechanics*, vol. 50, iss. 6, pp. 627–636. https://doi.org/10.1007/s10778-014-0661-7
3. Guz, A. N., Kubenko, V. D., & Cherevko, M. A. (1978). *Difraktsiya uprugikh voln* [Diffraction of elastic waves]. Kiyev: Naukova Dumka, 307 p. (in Russian).
4. Grinchenko, V. T. & Meleshko, V. V. (1981). *Garmonicheskiye kolebaniya i volny v uprugikh telakh* [Harmonic oscillations and waves in elastic bodies]. Kiyev: Naukova Dumka, 284 p. (in Russian).
5. Grinchenko, V. T. & Ulitko, A. F. (1968). An exact solution of the problem of stress distribution close to a circular hole in an elastic layer. *Soviet Applied Mechanics*, vol. 4, iss. 10, pp. 31 – 37. https://doi.org/10.1007/BF00886618
6. Grinchenko, V. T. & Ulitko, A. F. (1985). *Prostranstvennyye zadachi teorii uprugosti i plastichnosti. Ravnovesiye uprugikh tel kanonicheskoy formy* [Spatial problems of the theory of elasticity and plasticity. Equilibrium of elastic bodies of canonical form]. Kiyev: Naukova Dumka, 280 p. (in Russian).
7. Volchkov, V. V., Vukolov, D. S., & Storozhev, V. I. (2016). *Difraktsiya voln sdviga na vnutrennikh tunnel'nykh tsilindricheskikh neodnorodnostyakh v vide polosti i vklyucheniya v uprugom sloye so svobodnymi granyami* [Diffraction of shear waves on internal tunnel cylindrical inhomogeneities in the form of a cavity and inclusion in the elastic layer with free face]. *Mekhanika tverdogo tela – Mechanics of Rigid Bodies*, vol. 46, pp. 119 – 133 (in Russian).
8. Nikolayev, A. G. & Protsenko, V. S. (2011). *Obobshchennyy metod Furye v prostranstvennykh zadachakh teorii uprugosti* [The generalized Fourier method in spatial problems of the theory of elasticity]. Kharkov: Nats. aerokosm. universitet im. N. Ye. Zhukovskogo «KHAI», 344 p. (in Russian).
9. Nikolayev, A. G. & Orlov, Ye. M. (2012). *Resheniye pervoy osesimmetrichnoy termouprugoy krayevoy zadachi dlya transversalno-izotropnogo poluprostranstva so sferoidalnoy polostyu* [Solution of the first axisymmetric thermoelastic boundary value problem for a transversely isotropic half-space with a spheroidal cavity]. *Problemy obchyslyuvalnoyi mekhaniky i mitsnosti konstruktsiy – Problems of computational mechanics and strength of structures*, vol. 20, pp. 253-259 (in Russian).
10. Miroshnikov, V. Yu. (2018). First basic elasticity theory problem in a half-space with several parallel round cylindrical cavities. *Journal of Mechanical Engineering*, vol. 21, no. 2, pp. 12–18.
11. Protsenko, V. & Miroshnikov, V. (2018). Investigating a problem from the theory of elasticity for a half-space with cylindrical cavities for which boundary conditions of contact type are assigned. *Eastern-European Journal of Enterprise Technologies*, vol. 4, no. 7, pp. 43–50. https://doi.org/10.15587/1729-4061.2018.139567
12. Nikolayev, A. G., Shcherbakova, A. Yu., & Yukhno, A. I. (2006). *Deystviye sosredotochennoy sily na transversalno-izotropnoye poluprostranstvo s paraboloidalnym vklyucheniyem* [Action of concentrated force on a transversely-isotropic half-space with paraboloidal inclusion]. *Voprosy proyektirovaniya i proizvodstva konstruktsiy letatelnykh apparatov – Questions of design and production of aircraft structures*, vol. 2, pp. 47–51 (in Russian).
13. Miroshnikov, V. Yu. (2018). Evaluation of the stress-strain state of half-space with cylindrical cavities. *Visnyk Dniprovskoho universytetu. Seriya: Mekhanika – Bulletin of the Dnipro University. Series: Mechanics*, vol. 26, no. 5, pp. 109–118.
14. Nikolayev, A. G. & Tanchik, Ye. A. (2013). *Raspredeleniye napryazheniy v yacheyke odnonapravlennogo kompozitsionnogo materiala, obrazovannogo chetyrmya tsilindricheskimi voloknami* [Stress distribution in a cell of a unidirectional composite material formed by four cylindrical fibers]. *Visnyk Odeskoho natsionalnoho universytetu. Matematyka. Mekhanika – Odesa National University Herald. Mathematics and Mechanics*, vol. 4, pp. 101–111 (in Russian).
15. Protsenko, V. S. & Ukrainets, N. A. (2015) *Primeneniye obobshchennogo metoda Fur'ye k resheniyu pervoy osnovnoy zadachi teorii uprugosti v poluprostranstve s tsilindricheskoy polostyu* [Application of the generalized Fourier method to the solution of the first main problem of the theory of elasticity in a half-space with a cylindrical cavity]. *Visnyk Zaporizkoho natsionalnoho universytetu – Visnyk of Zaporizhzhya National University,* vol. 2, pp. 193–202 (in Russian).
16. Solyanik-Krasa, K. V. (1987). *Osesimmetrichnaya zadacha teorii uprugosti* [Axisymmetric problem of the theory of elasticity]. Moscow: Stroyizdat, 336 p. (in Russian).


*Received 21 March 2019*

**Дослідження напружено-деформованого стану шару з повздовжньою циліндричною товстостінною трубою та заданими на межах шару переміщеннями**

**Мірошніков В. Ю.**

Харківський національний університет будівництва та архітектури, 61002, Україна, м. Харків, вул. Сумська, 40

*Запропоновано аналітико-числовий підхід до розв'язання просторової задачі теорії пружності для шару з круговою циліндричною трубою. Циліндрична порожня товстостінна труба розташована всередині шару паралельно його поверхням та жорстко з ним скріплена. Необхідно дослідити напружено-деформований стан пружних тіл шару та труби. На внутрішній поверхні труби задані напруження, на межах шару – переміщення. Розв'язок просторової задачі теорії пружності отримано узагальненим методом Фур'є стосовно системи рівнянь Ламе в циліндричних координатах, пов'язаних із трубою, та в декартових координатах, пов'язаних із межами шару. Нескінченні системи лінійних алгебраїчних рівнянь, які отримані в результаті задовольняння граничних умов та умов сполучення, розв'язано методом зрізання. В результаті отримані переміщення та напруження в різних точках пружного шару та пружної труби. Завдяки підібраному параметру зрізання для заданих геометричних характеристик виконання граничних умов доведено до $10^{-3}$. Проведено аналіз напружено-деформованого стану тіла за різних товщин труби, а також за різних відстаней від труби до меж шару. Подані графіки нормальних та дотичних напружень на межі труби та шару, а також нормальні напруження на внутрішній поверхні труби. Вказані графіки напружень свідчать про те, що у разі наближення труби до верхньої межі шару напруження в тілі шару та в тілі труби зростають, у разі зменшення товщини труби напруження в тілі шару зменшуються, а в тілі труби зростають. Запропонований метод може використовуватись для розрахунку конструкцій та деталей, розрахункові схеми яких співпадають з постановкою задачі даної роботи. Наведений аналіз напруженого стану може бути використаний для підбору геометричних параметрів конструкції, що проектується, а графік напружень на межі труби та шару – для аналізу міцності з'єднання.*

***Ключові слова:*** *товстостінна труба в шарі, рівняння Ламе, узагальнений метод Фур'є.*

## Література

1. Vaysfel'd N., Popov G., Reut V. The axisymmetric contact interaction of an infinite elastic plate with an absolutely rigid inclusion. *Acta Mech.* 2015. Vol. 226. P. 797–810. https://doi.org/10.1007/s00707-014-1229-7
2. Попов Г. Я., Вайсфельд Н. Д. Осесимметричная задача теории упругости для бесконечной плиты с цилиндрическим включением при учете ее удельного веса. *Прикл. механика*. 2014. Т. 50. № 6. С. 27–38.
3. Гузь А. Н., Кубенко В. Д., Черевко М. А. Дифракция упругих волн. Киев: Наук. думка, 1978. 307 с.
4. Гринченко В. Т., Мелешко В. В. Гармонические колебания и волны в упругих телах. Киев: Наук. думка, 1981. 284 с.
5. Grinchenko V. T., Ulitko A. F. An exact solution of the problem of stress distribution close to a circular hole in an elastic layer. *Soviet Appl. Mechs*. 1968. No. 10. P. 31–37. https://doi.org/10.1007/BF00886618
6. Гринченко В. Т., Улитко А. Ф. Пространственные задачи теории упругости и пластичности. Равновесие упругих тел канонической формы. Киев: Наук. думка, 1985. 280 с.
7. Волчков В. В., Вуколов Д. С., Сторожев В. И. Дифракция волн сдвига на внутренних туннельных цилиндрических неоднородностях в виде полости и включения в упругом слое со свободными гранями. *Механика твердого тела*. 2016. Вып. 46. С. 119–133.
8. Николаев А. Г., Проценко В. С. Обобщенный метод Фурье в пространственных задачах теории упругости. Харьков: Нац. аэрокосм. ун-т им. Н. Е. Жуковского «ХАИ», 2011. 344 с.
9. Николаев А. Г., Орлов Е. М. Решение первой осесимметричной термоупругой краевой задачи для трансверсально-изотропного полупространства со сфероидальной полостью. *Проблеми обчислювальної механіки і міцності конструкцій*. 2012. Вип.20. С. 253–259.
10. Miroshnikov V. Yu. First basic elasticity theory problem in a half-space with several parallel round cylindrical cavities. *J. Mech. Eng.* 2018. Vol. 21. No. 2. P. 12–18.
11. Protsenko V., Miroshnikov V. Investigating a problem from the theory of elasticity for a half-space with cylindrical cavities for which boundary conditions of contact type are assigned. *Eastern-European J. Enterprise Techn. Appl. Mech.* 2018. Vol. 4. No. 7. P. 43–50. https://doi.org/10.15587/1729-4061.2018.139567
12. Николаев А. Г., Щербакова А. Ю., Юхно А. И. Действие сосредоточенной силы на трансверсально-изотропное полупространство с параболоидальным включением. *Вопр. проектирования и пр-ва конструкций летат. аппаратов. Сб. науч. тр. Нац. аерокосм. ун-та им. Н. Е. Жуковского «ХАИ»*. 2006. Вып. 2. С. 47–51.
13. Miroshnikov V. Yu. Evaluation of the stress-strain state of half-space with cylindrical cavities. *Visnyk Dniprovskoho universytetu. Ser. Mekhanika – Bulletin of the Dnipro University*. 2018. Vol. 26. No. 5. P. 109–118.
14. Николаев А. Г., Танчик Е. А. Распределение напряжений в ячейке однонаправленного композиционного материала, образованного четырьмя цилиндрическими волокнами. *Вісн. Одес. нац. ун-ту. Математика. Механіка*. 2013. Т.18, Вип. 4(20). С. 101–111.
15. Проценко В. С., Украинец Н. А. Применение обобщенного метода Фурье к решению первой основной задачи теории упругости в полупространстве с цилиндрической полостью. *Вісн. Запоріз. нац. ун-ту*. 2015. Вып. 2. С. 193–202.
16. Соляник-Краса К. В. Осесимметричная задача теории упругости. М.: Стройиздат, 1987. 336с.